RSC Advances

PAPER

View Article Online
View Journal | View Issue

Cite this: *RSC Adv.*, 2023, **13**, 24801

Reservoir computing with the electrochemical formation and reduction of gold oxide in aqueous solutions with a three-electrode electrochemical setup†

Ryo Yamada, Shuto Watanabe and Hirokazu Tada*

Received 11th July 2023
Accepted 14th August 2023

DOI: 10.1039/d3ra04614a

rsc.li/rsc-advances

Supervised classification of handwritten digits *via* physical reservoir computing (PRC) using electrochemistry with a three-electrode electrochemical setup was demonstrated. Short-term memory required for the PRC was realized for 3 bit pulse patterns by adjusting the formation/reduction ratio of gold oxides, showing a wide potential of electrochemistry as resources of PR devices.

Machine learning based on neural networks (NN) has been used for information processing.[1] However, some disadvantages of NN are the high cost of computational resources and the long training process. To overcome these limitations, physical reservoir computing (PRC) was proposed.[2] In PRC, signals are fed to PR devices that produce non-linear responses and short-term memory for input history. The outputs of the PR devices will be used as the input of the NN or a simpler network for the machine learning process.

PRC is expected to cost less than conventional NN systems because fewer layers of NNs are required. To date, PR devices have been proposed using optical circuits,[3] dielectric relaxation in ferroelectrics,[4] spin relaxation,[5] and solid-state redox reactions.[6,7] To produce the characteristics required for PR devices, redox reactions in the liquid phase, that is, electrochemistry in solutions, are useful because many non-linear phenomena appear in simple electrochemical setups.[8,9]

PR devices are also expected to be used as so-called edge computing devices because they can convert input signals into signals more suitable for machine learning in real time. For this purpose, time responses of PR devices should match those of the signals to be processed. The time response of PR by electrochemistry can be tuned by various parameters such as choice of reactions, concentration, temperature and hydrodynamics of solution in electrochemical cell. This wide capability would make electrochemistry as attractive and useful resource for PR devices.

Several studies have reported the use of charging of electrical double layers,[10] redox reactions in solutions,[11,12] and formation of complex network structures.[13,14] However, the relationship between electrochemical reactions and PR properties has not been fully understood, even though it is essential for the rational design of electrochemical PR devices.

In the earlier studies, the voltage was applied to the two electrodes in solution. In this two-terminal configuration, control and analysis of the redox reactions are unreliable because the electrochemical potentials of the electrodes are not controlled. To overcome this problem, a three-electrode configuration was proposed,[15] and used as a standard technique for electrochemical measurements. In brief, the three-electrode configuration uses working (WE), counter (CE), and reference (RE) electrodes. The WE is where the electrochemical reactions of interest take place, whereas the electrochemical potential of the WE (E_W) is controlled with respect to the RE whose electrochemical potential is determined by the equilibrium of the redox reactions occurring on the surface of the RE. Meanwhile, the potential difference between the WE and CE is controlled such that the potential difference between the WE and RE matches the desired value to cause the electrochemical reactions. The potential regulation is conducted using a device called potentiostat. With this configuration, the hysteresis in the oxidation and reduction processes can be effectively used because the electrical current (I) due to the oxidation and reduction can be distinguished.

In this study, we demonstrate PRC using the electrochemical formation and reduction of gold-oxide (herein referred to as *Au oxidation–reduction* for the simplicity while the reaction consists of several steps and multiple products) in aqueous solutions[16,17] with a standard three-electrode electrochemical setup. *Au oxidation–reduction* is easily reproducible because the gold-oxide remains on the surface of electrodes and characteristics of reactions are relatively insensitive to the structure of electrochemical cell and configuration of electrodes. These characteristics makes *Au oxidation–reduction* a good model system.

Division of Frontier Materials Science, Graduate School of Engineering Science, Osaka University, Toyonaka, Osaka, 560-8531, Japan. E-mail: tada.hirokazu.es@osaka-u.ac.jp

† Electronic supplementary information (ESI) available. See DOI: https://doi.org/10.1039/d3ra04614a

Short-term memory is realized and tuned by adjusting the oxidation and reduction processes involved during the pulse signal transduction. An image classification task is demonstrated as an application example.

Au oxidation–reduction was conducted in $HClO_4$ aqueous solutions using gold wires (1 mm in diameter and *ca.* 0.5 cm in length immersed in the solution) as the WE and CE. A gold wire covered with gold-oxide was used as the RE. The solution was bubbled with N_2 to remove residual air before the experiment to avoid side reactions owing to O_2 in the solutions.

Voltage waveforms were generated by a 16 bit-digital-to-analog converter and fed into a potentiostat. The electrical current signals were recorded using a 16 bit-analog-to-digital converter. For image classification, a dataset from the Modified National Institute of Standards and Technology (MNIST)[18] was used as the learning and test data. To create the NN layer for PRC, an open-source neural network library (Keras[19]) was used. Detailed information is provided in the ESI.†

Fig. 1 shows a cyclic voltammogram (CV) of the gold electrode in a 0.1 mM $HClO_4$ solution at 300 mV s^{-1}. A positive (cathodic) current corresponding to the formation of gold-oxide on the electrode is observed at $E_W >$ *ca.* −0.1 V when E_W is started from the potential at which gold-oxide is completely reduced. Meanwhile, a negative (anodic) current corresponding to the reduction of gold-oxide remained on the electrode is observed at *ca.* $-0.1\ V > E_W > -0.5$ V when E_W was scanned in the negative direction after the formation of gold-oxide.[16,17] These reactions are repeatable by the cyclic sweep of E_W.

From Fig. 1, it can be deduced that the E_W and I have a nonlinear relationship and hysteresis. The three-electrode configuration enables us to distinguish electrical current due to the formation of gold-oxide and reduction of it and use them as independent signals.

To test short-term memory, we measured the current response of the voltage pulse signals for [001] and [101]. The pulse signals, "1" and "0", are represented as $E_W = 0.3$ V and 0.0 V, respectively. Under these conditions, gold-oxide formation begins at "1" whereas reduction begins at "0" when the gold-oxide existed on the surface. E_W was set to −0.4 V for 1 s before and after the application of each pulse pattern to remove the gold-oxide produced by the application of signals.

Fig. 2a and b show the pulse signals for [001] and [101], respectively. Fig. 2c shows I transients for the both signals. Sharp increments followed by smooth decays of I are observed for the voltage steps at 0.2 s. In the decay region, I for [001] is larger than that for [101]. This result indicates that [101] and

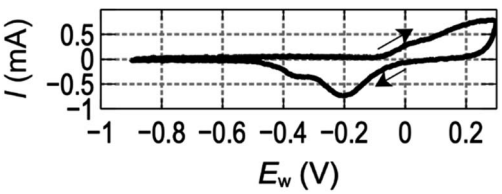

Fig. 1 Cyclic voltammogram of a gold electrode in 0.1 mM $HClO_4$ aqueous solution taken at 300 mV s^{-1}.

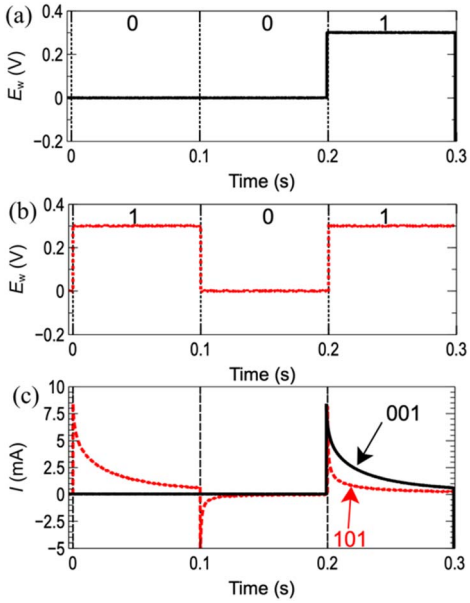

Fig. 2 3 bit-pulse inputs for (a) [001] and (b) [101]. (c) Current transients for [001] (black) and [101] (red, dotted line).

[001] can be distinguished from the decay of I in the final pulse, suggesting that the decay of I may contain information for 3 bit.

The initial sharp increase of I was attributed to the rearrangement of ions at the interface caused by the electric field, *i.e.*, formation of electrical double layer. The following decay of I is attributed to formation of gold-oxide because this decay was not observed when *Au oxidation–reduction* was not involved in the pulse potentials (Fig. S1 in ESI†).

While the formation process of gold-oxide contains several steps,[16,17] the current decay during the pulse volage representing "1" can be explained as follows: the formation of gold-oxide is suppressed on the surface where the gold oxide was already formed because replacement of gold atoms is required for the further formation of gold-oxide. As the gold-oxide formation proceeds, area of bare-gold surface, hence, the oxidation current is decreased.

The difference in the decays of I between [001] and [101] can be qualitatively explained as follows: When [101] is applied, gold-oxide is formed at the initial input of "1". The gold-oxide is partially reduced in the subsequent input, "0". Therefore, at the final input, "1", gold-oxide is formed on the surface which has already been partially covered with gold-oxide. This results in a lower I than that for [001] in which gold-oxide is formed on a bare gold surface. The gold-oxide left on the surface is essential to produce the difference in the decays of I as no difference was observed when the gold-oxide was completely reduced at [0] as shown in Fig. S2 in ESI.†

We examined if recognition of all 3 bit patterns is possible from the decay of I. The average current from 0.26 s to 0.29 s is used as an output of the PR (I_{out}). Fig. 3 shows the average I_{out} of 50 measurements for all 3 bit patterns normalized by I_{out} for [001] (I_{001}) where Au oxidation took place on the bare-gold surface resulting in the largest value. More detailed statistical

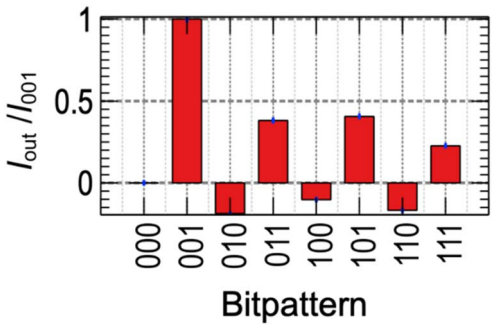

Fig. 3 Average of I_{out} for 3 bit patterns.

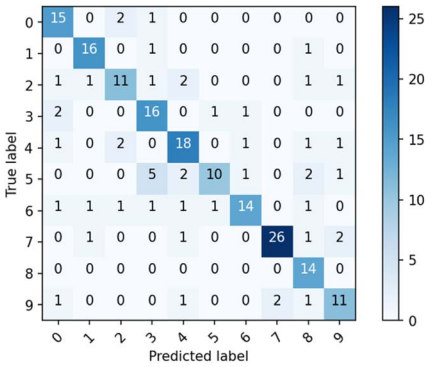

Fig. 4 A summary of one the results of image classification task.

information is shown in ESI.† It was observed that all 3 bit patterns result in different I_{out}. This result indicates I_{out} contains information for 3 bits, which is considered as the short-term memory.

The positive (negative) value was observed for the patterns ended with "1" ("0"), indicating the oxidation (reduction) process dominates the signal, except "000" where no reaction took place. The dependence of I_{out} for the 3 bit patterns depends on the pulse voltage are shown in Fig. S4 and S5 in ESI,† showing ability to tune the response.

We conducted an image classification task using the current transient observed according to a previously reported procedure.[10,20,21] The details are provided in the ESI.† In brief, images of handwritten numbers taken from the MNIST database were converted into a one-dimensional binary array, that is, a pulse train. The pulse train was then applied to the electrochemical cell every three pulses and I_{out} was measured. The I_{out} was then fed to the input nodes of the NN layer. Supervised learning was conducted using I_{out} obtained from the 1000 image sets in the training data sets and classification was tested using I_{out} obtained from 201 data sets which are not used in the learning process. See ESI† for more details. The experiment was carried out in a 1.0 M $HClO_4$ solution, in which a faster current transient was obtained (Fig. S6 in ESI†). Before the experiment, *Au oxidation–reduction* was repeated until the CV traces became identical so that changes in the roughness of the electrode owing to *Au oxidation–reduction* would not affect I_{out}. Before the pulse input, the E_W was set to −0.4 V for 0.1 s to reduce gold-oxides on the WE generated by pulse.

Fig. 4 shows one of the results of image classification task. The column ("Predicted label") represents the count of the digit predicted by the classification. The row ("True label") represents the true digit written in the image.

For example, when the true digit written in the images is "4", the count for the correct classification (18) is found at (4,4). The counts for the wrong classification (6 in total) are found at (4,0), (4,2), (4,6), (4,8) and (4,9). The accuracy of the classification is evaluated by ratio of count for correct classification to the total number of images tested.

From this matrix, we concluded that image classification task was successful because the highest counts were obtained at the true values for all the numbers tested with the total accuracy of 76% which is obtained from the average of 10 entire learning process to eliminate the variability for each learning process. The accuracy would be affected by the fluctuation of I_{out} due to the instability of the environment such as temperature and vibrations and subtle dissolution of gold and gold-oxide in the huge number of reaction cycles[17] and would be improved by optimizing the conditions for the reactions.

Conclusions

We demonstrated PRC based on the electrochemical formation and reduction of gold-oxides. The PR properties were achieved and tuned through appropriate electrochemical reactions using a three-electrode electrochemical setup. This result indicates that electrochemistry with three-electrode setup has huge potential for studies of PR devices.

Author contributions

Ryo Yamada and Hirokazu Tada contributed equally to this work. Ryo Yamada: conceptualization (equal); investigation (equal), writing original draft. Shuto Watanabe: investigation (equal). Hirokazu Tada: conceptualization (equal), funding acquisition, supervisions, writing – review.

Conflicts of interest

There are no conflicts to declare.

Acknowledgements

This work was supported by JSPS KAKENHI Grant Number 22H00315 and Core-to-Core Program (grant number: JPJSCCA20220006).

Notes and references

1 S. Samarasinghe, *Neural Networks for Applied Sciences and Engineering: From Fundamentals to Complex Pattern Recognition*, CRC Press, 2016.
2 G. Tanaka, T. Yamane, J. B. Héroux, R. Nakane, N. Kanazawa, S. Takeda, H. Numata, D. Nakano and A. Hirose, *Neural Networks*, 2019, **115**, 100–123.

3 D. Brunner, B. Penkovsky, B. A. Marquez, M. Jacquot, I. Fischer and L. Larger, *J. Appl. Phys.*, 2018, **124**, 152004.
4 E. Nako, K. Toprasertpong, R. Nakane, Z. Wang, Y. Miyatake, M. Takenaka and S. Takagi, in *2020 IEEE Symposium on VLSI Technology*, 2020, pp. 1–2.
5 J. Torrejon, M. Riou, F. A. Araujo, S. Tsunegi, G. Khalsa, D. Querlioz, P. Bortolotti, V. Cros, K. Yakushiji, A. Fukushima, H. Kubota, S. Yuasa, M. D. Stiles and J. Grollier, *Nature*, 2017, **547**, 428–431.
6 M. Nakajima, K. Minegishi, Y. Shimizu, Y. Usami, H. Tanaka and T. Hasegawa, *Nanoscale*, 2022, **14**, 7634–7640.
7 Y. Usami, B. van de Ven, D. G. Mathew, T. Chen, T. Kotooka, Y. Kawashima, Y. Tanaka, Y. Otsuka, H. Ohoyama, H. Tamukoh, H. Tanaka, W. G. van der Wiel and T. Matsumoto, *Adv. Mater.*, 2021, **33**, e2102688.
8 M. T. M. Koper, *J. Chem. Soc., Faraday Trans.*, 1998, **94**, 1369–1378.
9 D. Kim and J.-S. Lee, *ACS Appl. Electron. Mater.*, 2023, **5**, 664–673.
10 S.-G. Koh, H. Shima, Y. Naitoh, H. Akinaga and K. Kinoshita, *Sci. Rep.*, 2022, **12**, 6958.
11 S. Kan, K. Nakajima, T. Asai and M. Akai-Kasaya, *Adv. Sci.*, 2022, **9**, e2104076.
12 T. Matsuo, D. Sato, S.-G. Koh, H. Shima, Y. Naitoh, H. Akinaga, T. Itoh, T. Nokami, M. Kobayashi and K. Kinoshita, *ACS Appl. Mater. Interfaces*, 2022, **14**, 36890–36901.
13 M. Cucchi, C. Gruener, L. Petrauskas, P. Steiner, H. Tseng, A. Fischer, B. Penkovsky, C. Matthus, P. Birkholz, H. Kleemann and K. Leo, *Sci. Adv.*, 2021, **7**, eabh0693.
14 G. Milano, G. Pedretti, K. Montano, S. Ricci, S. Hashemkhani, L. Boarino, D. Ielmini and C. Ricciardi, *Nat. Mater.*, 2022, **21**, 195–202.
15 A. J. Bard, L. R. Faulkner and H. S. White, *Electrochemical Methods: Fundamentals and Applications*, John Wiley & Sons, 2022.
16 L. D. Burke and P. F. Nugent, *Gold Bull.*, 1997, **30**, 43–53.
17 S. Cherevko, A. A. Topalov, A. R. Zeradjanin, I. Katsounaros and K. J. J. Mayrhofer, *RSC Adv.*, 2013, **3**, 16516–16527.
18 The MNIST DATABASE, **https://yann.lecun.com/exdb/mnist/index.html**.
19 Keras, **https://keras.io/**.
20 C. Du, F. Cai, M. A. Zidan, W. Ma, S. H. Lee and W. D. Lu, *Nat. Commun.*, 2017, **8**, 2204.
21 R. Midya, Z. Wang, S. Asapu, X. Zhang, M. Rao, W. Song, Y. Zhuo, N. Upadhyay, Q. Xia and J. J. Yang, *Adv. Intell. Syst.*, 2019, **1**, 1900084.